

Gradient descent reliably finds depth- and gate-optimal circuits for generic unitaries

Alex Meiburg^{1,2} and Janani Gomathi^{1,3}

¹Perimeter Institute for Theoretical Physics

²Institute for Quantum Computing, University of Waterloo

³Institute for Information Processing (tnt/L3S), Leibniz Universität Hannover, Germany

When the gate set has continuous parameters, synthesizing a unitary operator as a quantum circuit is always possible using exact methods, but finding minimal circuits efficiently remains a challenging problem. The landscape is very different for *compiled* unitaries, which arise from programming and typically have short circuits, as compared with *generic* unitaries, which use all parameters and typically require circuits of maximal size. We show that simple gradient descent reliably finds depth- and gate-optimal circuits for generic unitaries, including in the presence of restricted chip connectivity. This runs counter to earlier evidence that optimal synthesis required combinatorial search, and we show that this discrepancy can be explained by avoiding the random selection of certain parameter-deficient circuit skeletons.

1 Introduction

Unitary synthesis refers to the task of decomposing a unitary operator, represented as a matrix, into a series of quantum gates natively supported by hardware in a quantum computer - typically, one- and two-qubit gates. This can be done deterministically using algorithms like Quantum Shannon Decomposition [16], but this will generally produce circuits that are far from optimal in size. Moreover, in general, finding an optimal decomposition is believed to be very hard [5, 8]. The correct notion of optimality is also context dependent, for instance, there are works which focus on synthesizing Clifford circuits with a low CNOT

Alex Meiburg: gdqcs@ohaithe.re

Janani Gomathi: jananirajagopal47@gmail.com

count, synthesizing Clifford+T circuits with a low T count [12, 15], or on accommodating limited hardware connectivity[11, 19].

In the setting where our available gate set includes real parameters (the gate set of arbitrary single-qubit unitaries + CNOT, for example), one approach is to posit a circuit "skeleton" of parameterized gates and then search over the real parameter space to minimize the error between the target and synthesized unitary. The resulting optimization problem is highly non-convex, but earlier works [2, 3], have shown some forms of success with gradient descent-based approaches, sometimes referred to as GRAPE [6, 9].

For unitaries that arise from logical programs, it is typical to expect a short circuit due to the presence of a particular structure or symmetry. But for a *generic* unitary on n -qubits, a circuit of depth $\Theta(4^n/n)$ is required, as given by parameter counting. This is the regime that we focus on: can we find a depth-optimal circuit that implements a generic unitary? Previous work [3] suggested that gradient descent could do this sometimes, but only with some probability that rapidly fell to zero as the number of qubits grew. In contrast, we find that – with one simple prescription for selecting the circuit skeleton – gradient descent is able to find a depth-optimal circuit every time. These circuits naturally turn out to be optimal in terms of the number of entangling gates, and in the number of total gates, as well.

Our investigations are empirical, but strongly suggest that gradient descent fails only when certain bad circuit skeletons are selected, resulting in an *effectively underparameterized* circuit. This is validated by further experiments on circuit topologies with connectivity constraints: gradient descent continued to find optimal-size circuits even in 1D or star-topology qubit layouts and never failed even across hundreds of trials. As a

result, we conjecture that the resulting loss landscape has no local minima, that is, no locally optimum circuit parameterization with a fidelity of less than 1.

2 Background

Usually, there are two kinds of optimizations that one does in the case of transforming unitaries into circuits. When the unitary is already given as a circuit, the goal is to find a shorter or hardware-compatible circuit; this process is typically referred to as "compiling". Meanwhile, "synthesis" typically refers to when the unitary is given as the full $2^n \times 2^n$ matrix [15, 3, 2]. A common algorithm that performs exact synthesis for 1-qubit systems is a version of the Kliuchnikov–Maslov–Mosca (KMM) algorithm [10] that uses algebraic number theory to break down a unitary into Clifford + T gates.

Moreover, there are many different existing approaches to unitary synthesis for larger systems. One of the recent methods in approximate synthesis uses the process of reinforcement learning (RL), and in this context, unitary synthesis is framed as a sequential decision-making problem in which the RL agent constructs a quantum circuit one gate at a time. While it is promising, a major disadvantage of this approach is that the training is often unitary-specific. Although some recent works propose robust or generalized training schemes [15], the approach remains difficult to scale to larger systems. Another decision-making approach used in unitary synthesis is Mixed-Integer Programming [13]. Here, hardware constraints, such as gate types and connectivity, are encoded as part of this problem. The objective is to determine an optimal circuit structure that implements the target unitary while respecting these constraints. Along with scalability issues, this method has the additional limitation that MIP problems are NP-hard problems at worst, which means that they may not be tractable in all cases.

Quantum compilers, such as the one provided by Qiskit, are responsible for transforming the entire high-level quantum algorithms into hardware executable circuits while satisfying the constraints of the target quantum device. This uses Quantum Shannon Decomposition [16], which gives a straightforward way to synthesize an ar-

bitrary unitary matrix into a circuit, but the resulting circuit can be far from optimal. In particular, the use of recursive decomposition means that it is not parameter-optimal, as there is no attempt to cancel out redundant parameters at each step. Various works have investigated algorithms to find shorter circuits, although the general problem is hard[5, 8]. Special cases include synthesizing Clifford circuits with a low CNOT count, synthesizing Clifford+T circuits with a low T count[15], or focusing on accommodating limited hardware connectivity[11, 19].

In our approach, we aim to develop a parameter-optimal method for unitary synthesis using gradient descent. We consider the unitary synthesis problem as, given an n -qubit unitary matrix $U \in \mathbb{C}^{2^n \times 2^n}$, to produce a decomposition into a prescribed gate set. Up to an irrelevant global phase, U has $4^n - 1$ real parameters, so if each individual gate has at most p real parameters, a minimum of $\lceil \frac{4^n - 1}{p} \rceil$ gates will be needed for a generic unitary. A majority of effort has focused on identifying structured unitaries that can do much better than this bound, but generic unitaries still play an important role for holding input parameters in quantum physics or chemistry simulations, e.g. [4, 1]. Accordingly, we focus on the generic case, where the main question is whether the $\lceil \frac{4^n - 1}{p} \rceil$ bound can be tightly achieved.

3 Problem Setup and Method

3.1 Parametrization

We aim to decompose any target unitary into a quantum circuit made of one-qubit and two-qubit gates, from a continuous gate set. We focus especially on the case where the CNOT gate is the unique two-qubit entangling gate, and arbitrary single-qubit unitaries are allowed, with three degrees of freedom each. Such a decomposition can be expressed as [2],

$$U_{circ} = S_\ell T_{\ell-1} \dots S_2 T_1 S_1 \quad (1)$$

Here each $S_i = U_1 \otimes U_2 \dots \otimes U_j \dots$, i.e., the tensor product of some single qubit unitaries, and the T_i is some set of simultaneous CNOT gates. We call each $S_i T_i$ a layer, the final layer being just S_ℓ , and we say this is an ℓ -layer decomposition of the unitary. Each single-qubit U_j is in turn

parameterized by the three Euler angles,

$$U_j(\theta_1, \theta_2, \theta_3) = R_z(\theta_2)R_y(\theta_1)R_z(\theta_3) \quad (2)$$

where $R_y(\theta) = \exp(-i\theta Y/2)$ and $R_z(\theta) = \exp(-i\theta Z/2)$. After fixing T_i , an appropriate circuit decomposition is sought by optimizing the parameters of these single-qubit unitaries so that the circuit implements the target unitary up to some precision. For useful quantum computing, an error (one minus fidelity F) in the range of $10^{-7} \sim 10^{-9}$ is a typical threshold; in our experiments, this is roughly the threshold of numerical error, and we assume that this indicates that there is indeed a perfect synthesis. Running with high precision numerics in a few cases seems to affirm this belief.

Each T_i is made up of an arrangement of CNOTs, for example $T_i = \text{CNOT}_{1 \rightarrow 3} \otimes \text{CNOT}_{2 \rightarrow 4} \dots$. Note that directionality is ultimately irrelevant, since $\text{CNOT}_{1 \rightarrow 2}$ and $\text{CNOT}_{2 \rightarrow 1}$ are equivalent under appropriate single-qubit transformations on either side. The pattern of CNOTs dictates what we call the "circuit skeleton", and as a discrete variable, it is held constant during gradient descent. Other works have considered searching over possible topologies, either by random search, brute-force enumeration, or relaxing the constraint to some continuous variable approximate constraint. In a sense, our main innovation is noticing that, for generic unitaries, this random search is unnecessary, and we can simply pick an ideal skeleton from the get-go using a simple design principle.

3.2 Cost Function

In order to perform gradient descent, we first define an appropriate cost function. Let the target unitary be U_{goal} and the unitary implemented by the quantum circuit be denoted by U_{circ} . For optimal parameters, we must find that

$$D = U_{\text{goal}}U_{\text{circ}}^\dagger \approx \mathbb{I} \quad (3)$$

up to a global phase.

Hence, the cost function must measure the deviation from \mathbb{I} up to a global phase, which is the distance between the two unitaries. For ease of computation, we choose the distance measure to be the trace distance. Therefore,

$$C = N - \text{abs}(\text{Tr}(D)) \quad (4)$$

where N is the dimension of the Hilbert space of our system. In accordance with the required precision, if $C \leq 10^{-8}$, we identify the decomposition of U_{circ} to be adequate for successful implementation of U_{goal} . We minimize the error C with simple gradient descent without momentum, and brief experimentation suggested that different gradient descent variants performed very comparably on this task. It was numerically advantageous to update each parameter sequentially as opposed to updating all variables in a batch, using a dynamical representation of the left and right parts of the circuit (similar to the "sweeping" typical in MPS calculations). This was the variant of gradient descent that was used in most experiments.

3.2.1 Approximation to the closest unitary through SVD

Seeking an acceleration to simple gradient descent, we consider skipping several steps of the descent process by singular value decomposition (SVD). To motivate this decision, note that optimizing the parameters in a single U_i is a unimodal optimization problem, and thus sufficiently many steps of gradient descent at one site will necessarily be equivalent to this SVD accelerator. The method is as follows. For any single-qubit unitary U_i that we optimize, we trace out the subsystem of interest, A_i , for each iteration. Then, we find the closest unitary to A_i through SVD [14]. This is some U_i such that the operator norm $\|A_i - U_i\|_2$ is minimized. The approximation goes as,

$$A_i = X \Sigma Y^\dagger \quad (5)$$

$$U_i = X Y^\dagger \quad (6)$$

where (5) is the SVD operation. The new unitary U_i is normalized so that we are still working with an $SU(2)$ matrix, and the Euler angles θ_1, θ_2 and θ_3 are extracted and stored.

In a mathematically precise sense, we can say that the SVD does not help escape local minima; it only accelerates the same computation that gradient descent could do anyway with an appropriate learning rate and site schedule. This acceleration avoids the need to pick a learning rate, and we can thus view this as a more manifold-aware optimization method.

3.2.2 Layer Calculation

During implementation, we need to calculate the size (equivalently, depth) of the required circuit. This is a straightforward exercise in parameter counting that we repeat here for clarity.

In a system with n qubits, the unitary U is $N \times N$, where $N = 2^n$, and has $P = N^2 - 1 = 4^n - 1$ real parameters. According to our earlier decomposition, we segment the circuit into layers $S_i C_i$ of alternating single-qubit unitaries and CNOTs. A general single-qubit unitary carries three free parameters, so each layer appears to contribute $3n$ parameters from the local gates. But then the symmetries of the CNOT gates reduce the overall parameter count. Specifically, a CNOT is invariant under (i) conjugation by Z rotation on the control, and (ii) conjugation by X rotation on the target, i.e.,

$$R_Z(\theta) \otimes I(CNOT)R_Z(\theta) \otimes I = \\ I \otimes R_X(\theta)(CNOT)I \otimes R_X(\theta) = CNOT.$$

These two symmetries effectively reduce 2 free parameters per CNOT.

One way of understanding this is that we could always choose to *normalize* a circuit according to the following procedure:

1. Writing each single qubit unitary in the first layer as $R_X(\theta_1)R_Y(\theta_2)R_Z(\theta_3)$ if it qubit will a control qubit in the next CNOT, or $R_X(\theta_1)R_Y(\theta_2)R_X(\theta_3)$ if it will be the qubit acted on by the CNOT. These are two different Euler angle decompositions.
2. Commute the last rotation (either R_Z or R_X) past the *CNOT*, altering the single-qubit unitaries in the second layer.
3. Proceed in this way for all layers, until the last, which is not followed by a CNOT.

Now all single-qubit unitaries have a canonical form with two real parameters, except for the last layer which has three real parameters, so that the total circuit with ℓ layers has $P = 2n(\ell-1) + 3n = (2\ell+1)n$ parameters. To express a generic unitary we then require $(2\ell+1)n \geq N^2 - 1$, or

$$\ell = \lceil \frac{4^n - 1 - n}{2n} \rceil. \quad (7)$$

An alternate calculation would say that each CNOT *loses* us two degrees of freedom; this symmetry can be calculated from the degeneracy of

its spectrum. Since CNOT has a spectrum of $\{-1, 1, 1, 1\}$, it has two degeneracies, which manifests as the loss of a two effective parameters. It is worth considering the parameter loss due to different two-qubit coupling gates:

- The CZ gate would have the same parameter loss of 2, as it is locally equivalent to CNOT.
- The Sycamore gate [7] has a spectrum $\{1, -i, i, \exp(-i\pi/6)\}$ and no degeneracies; no effective parameters are lost. This is also true for a generic two-qubit gate.
- The SWAP gate has only two degeneracies in the spectrum, but it also fails to mix the left- and right-symmetric subspaces, leading to a total loss of six real parameters. This means that *all* parameters from a layer of unitaries are lost, and, of course, $SU(2) + \text{SWAP}$ is not universal for computation.

In section 4.3 we discuss restricted circuit topologies, where we cannot make use of every qubit in every layer. Then the layer calculation is slightly altered.

4 Results

The primary question we wanted to investigate was regarding the reliability of the gradient descent method in optimization – and secondarily, its efficiency. The "cleanest" topology to study first was an even number of qubits in fully connected hardware, where we can exactly fill each layer of CNOTs with arbitrary connectivity. Therefore, we investigate our method for such two-qubit, four-qubit and six-qubit systems. In this section, we first describe the circuit decompositions for all system sizes. In particular, we elaborate on the importance and reasoning behind the choice of circuit topologies in bigger systems. Following that, we present the primary results we obtained by running the numerics across these different system sizes. Finally, we conclude this section with systems that do not have full connectivity and present conclusions on the effect of these constraints on the results.

4.1 Circuit decomposition and choice of topology

We demonstrate the choice of circuit design with two, four and six-qubit systems.

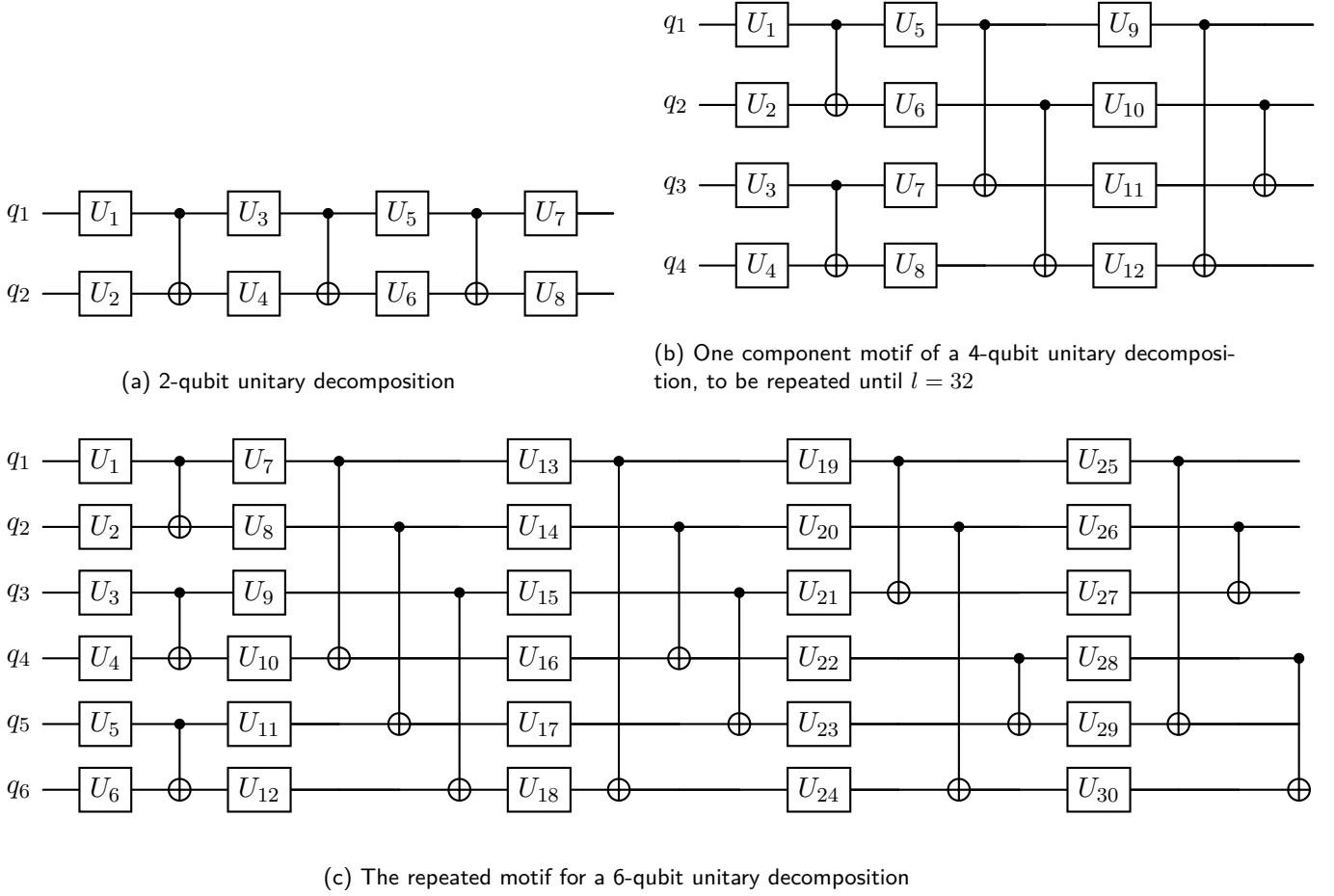


Figure 1: Circuit decompositions for 2-, 4-, and 6-qubit unitaries.

The two-qubit unitary needs three layers for adequate parameterization according to 7, and for that, there is a unique topology (see figure 1a). This is of course well-studied, and indeed an optimal and exact decomposition of a two-qubit unitary is known, see e.g. [17, 18].

Moving on to the four-qubit unitary, which needs 32 layers according to 7, and we now have a nontrivial question of picking the topology. Our first naïve strategy was to simply repeat the motif in 1b.

Why this motif? Up to permutations of qubits, it is the *unique* three-layer motif that directly connects all the qubits in the system to each other.

1. (1,2), (3,4)
2. (1,3), (2,4)
3. (1,4), (2,3)

Believing that good mixing would be necessary for good trainability of the circuit, we wanted to

avoid repeating a connection, so after these three pairings have been done, we go back to the least-recently used – and repeat the cycle of three. This decision turned out to be fortuitous, and likely optimal!

For six-qubit unitaries, we need $\ell = 341$, according to 7. The choice of topology for this case is quite non-trivial. Here, we have ${}^6C_2 = 15$ ways of picking out the pair of qubits for the CNOTs to act on in each layer. The order of these CNOTs becomes important in the decomposition, as certain patterns in the choice of subsystems can end up effectively reducing the number of parameters.

Let us elaborate on such a scenario with an example. Consider that the same two qubits are paired together for four layers consecutively, that is, three rounds of CNOT pairings. Here, we end up using $3 \cdot 8 - 2 \cdot 3 = 18$ parameters to build what is effectively a unitary that acts only on two qubits. However, a general two-qubit unitary requires just 15 parameters. The surplus parameters introduce redundancies in the circuit, lead-

ing to symmetries, i.e., directions in parameter space along which the output unitary remains unchanged. These symmetries reduce the number of effective degrees of freedom available to the rest of the circuit. As a result, the system will not have enough parameters and will not converge, despite appearing to have an adequate number of layers. This ultimately means that there are certain CNOT configurations for which the circuit will fail to converge.

In [3], this probability of failure, or rather the percentage of configurations that converge, was found through brute-force, random combinatorial search. The failed configurations are likely cases of effective underparameterization as described above. We give further numerical justification of this belief in Appendix D.

We made a more detailed investigation on the underparameterized regime of circuits for the bigger systems — four-qubit and six-qubit systems (see Appendix B). This was considered in an effort to reduce the CNOT count further. On examining the effect of this condition on convergence, we observe that the cost function plateaus much before the desired precision is reached, even when the number of layers is only slightly short of the required number. As the benefit in the reduction of gates does not compensate well enough for the loss in precision, we conclude that underparameterization is not very useful.

We continue to follow the logic that to ensure convergence, we require rapid mixing, with no reduction in the number of parameters. One way to do this is to make sure that each combination of CNOT pairing is only repeated in the circuit skeleton as far away as possible. Now, we must find the maximum number of other such combinations that can be inserted before repetition becomes inevitable. This problem is a well-known graph theory problem, referred to as the 1-factorization of a k -node graph. The maximum number of combinations corresponds to the number of 1-factors, which is given by $k - 1$. In the case of six nodes, this gives five such combinations. These five combinations are listed below.

1. (1,2), (3,4), (5,6)
2. (1,4), (2,5), (3,6)
3. (1,6), (2,4), (3,5)
4. (1,3), (2,6), (4,5)

5. (1,5), (2,3), (4,6)

It is important to note that this set of combinations is not unique, especially when the number of nodes is large. As before, after these five pairings, the CNOTs are repeated throughout the circuit in this order. This circuit is shown in figure 1c.

4.2 Numerics

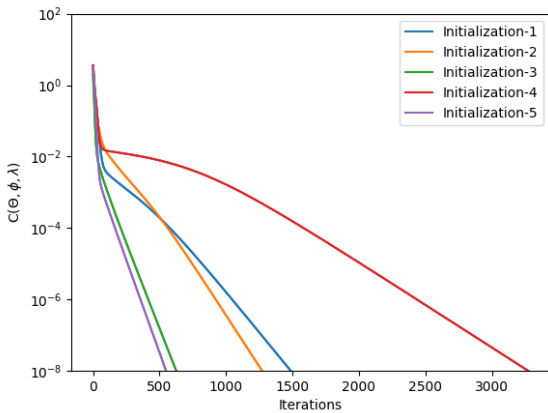
After considering the choice of circuit topologies, the optimization algorithm was run for around 200 two-qubit, 100 four-qubit and 30 six-qubit unitaries. Here we note that the results stated in this paper held without fail for all of these trials. The target unitaries for all system sizes were generated Haar-randomly using a function from the `scipy` library. During the runs, we optimized the parameters of the single-qubit unitaries using gradient descent for the following cases: (a) arbitrary target unitaries, (b) the same random target unitary with the decomposition initialized with different sets of parameters.

We observed that the circuit reliably converges in both cases, avoiding any local minima. Although certain initializations lead to faster convergence than others, this does not affect the overall consistency in convergence. Hence, we proceeded with random initialization for all subsequent runs. These findings are illustrated in figure 2a and figure 2b. Even as the system size increases, i.e. for four-qubit and six-qubit systems, these results continued to hold (see appendix A).

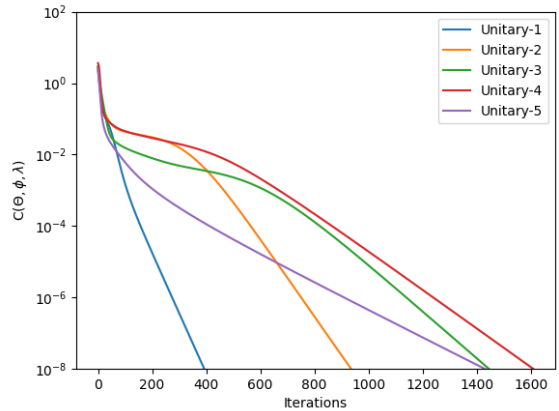
4.3 Handling Connectivity Constraints

So far, all the circuit topologies we have considered assume full qubit connectivity. However, practical quantum hardware typically imposes connectivity constraints that limit the combination of qubits that can be directly entangled. To evaluate the performance of our method under such conditions, we now examine circuits with restricted connectivity. Despite the connectivity constraints, both cases show reliable convergence with sufficient parameterization, while underparameterized circuits cause the cost function to plateau (see appendix C).

This means that we have obtained a parameter-optimal method for generic unitary synthesis in the case of circuits with low connectivity. This



(a) Convergences of the same 4×4 target unitary initialized with five different parameter sets. The y-axis is in log scale.



(b) Convergences of five random 4×4 target unitaries optimized using the gradient-based algorithm. The y-axis is in log scale.

Figure 2: Comparison of convergence behavior for different initializations (left) and different target unitaries (right).

is especially advantageous over alternative methods of unitary synthesis, such as general-purpose quantum compilers or exact synthesis techniques, which are not parameter-optimal. Further, one can expect the quantum compilers to give a circuit with a higher number of parameters and CNOT count due to the suboptimal decomposition methods they use. Another advantage of this method is that it works even when the actions of the target unitaries are not specified for all states. One can still measure the cost function for the subset of specified actions and perform gradient descent-based optimization for them.

5 Conclusion

Optimization via gradient descent has been found to converge reliably as long as there is adequate parameterization. As expected, circuits operating in the underparameterized regime exhibit reach a minimum in the cost function and fail to achieve perfect precision, but disappointingly this precision is too low to be useful; it is possible that more advanced optimization methods can find higher-accuracy decompositions. For larger systems, the choice of CNOT configuration becomes increasingly important: symmetries between layers can reduce the effective number of parameters, thereby hindering convergence. Nevertheless, the method remains robust even under limited connectivity, making it particularly well-suited to be used on realistic quantum hardware.

In addition, this method offers a practical and efficient framework for unitary synthesis in contrast to alternatives such as exact synthesis algorithms, which assume full connectivity, or standard quantum compilers, which may not yield parameter-efficient circuits.

6 Acknowledgements

We thank David Gosset for his support and insights. JG also sincerely thanks Keshav Das Agarwal for many fruitful discussions.

Research at Perimeter Institute is supported in part by the Government of Canada through the Department of Innovation, Science and Industry Canada and by the Province of Ontario through the Ministry of Colleges and Universities. Both authors were supported by Discovery Grant No. RGPIN-2019-0419.

References

- [1] Juan Miguel Arrazola, Olivia Di Matteo, Nicolás Quesada, Soran Jahangiri, Alain Delgado, and Nathan Killoran. Universal quantum circuits for quantum chemistry. *Quantum*, 6(742):742, June 2022.
- [2] Sahel Ashhab, Naoki Yamamoto, Fumiki Yoshihara, and Kouichi Sembra. Numerical analysis of quantum circuits for state preparation and unitary operator synthesis. *Phys. Rev. A (Coll. Park.)*, 106(2), August 2022.

[3] Sahel Ashhab, Fumiki Yoshihara, Miwako Tsuji, Mitsuhsa Sato, and Kouichi Sembra. Quantum circuit synthesis via a random combinatorial search. *Phys. Rev. A (Coll. Park.)*, 109(5), May 2024.

[4] Herschel A. Chawdhry and Mathieu Pellen. Quantum algorithms for the simulation of qcd processes in the perturbative regime, 2024.

[5] Nai-Hui Chia, Chi-Ning Chou, Jiayu Zhang, and Ruizhe Zhang. Quantum meets the minimum circuit size problem. 2021.

[6] P. de Fouquieres, S.G. Schirmer, S.J. Glaser, and Ilya Kuprov. Second order gradient ascent pulse engineering. *Journal of Magnetic Resonance*, 212(2):412–417, 2011.

[7] Matthew P. Harrigan et al. Quantum approximate optimization of non-planar graph problems on a planar superconducting processor. *Nature Physics*, 17(3):332–336, 2021.

[8] John M Hitchcock and A Pavan. On the NP-completeness of the minimum circuit size problem, December 2015.

[9] Navin Khaneja, Timo Reiss, Cindie Kehlet, Thomas Schulte-Herbrüggen, and Steffen J Glaser. Optimal control of coupled spin dynamics: design of NMR pulse sequences by gradient ascent algorithms. *J. Magn. Reson.*, 172(2):296–305, February 2005.

[10] Vadym Kliuchnikov, Dmitri Maslov, and Michele Mosca. Fast and efficient exact synthesis of single qubit unitaries generated by clifford and t gates, 2013.

[11] Gushu Li, Yufei Ding, and Yuan Xie. Tackling the qubit mapping problem for NISQ-era quantum devices. In *Proceedings of the Twenty-Fourth International Conference on Architectural Support for Programming Languages and Operating Systems*, pages 1001–1014, New York, NY, USA, April 2019. ACM.

[12] Michele Mosca and Priyanka Mukhopadhyay. A polynomial time and space heuristic algorithm for t-count. 2020.

[13] Harsha Nagarajan, Owen Lockwood, and Carleton Coffrin. Quantumcircuitopt: An open-source framework for provably optimal quantum circuit design, 2021.

[14] Yihui Quek and Patrick Rebentrost. Fast algorithm for quantum polar decomposition and applications. *Phys. Rev. Res.*, 4(1), February 2022.

[15] Sebastian Rietsch, Abhishek Y Dubey, Christian Utrecht, Maniraman Periyasamy, Axel Plinge, Christopher Mutschler, and Daniel D Scherer. Unitary synthesis of Clifford+T circuits with reinforcement learning. In *2024 IEEE International Conference on Quantum Computing and Engineering (QCE)*, pages 824–835. IEEE, September 2024.

[16] V V Shende, S S Bullock, and I L Markov. Synthesis of quantum-logic circuits. *IEEE Trans. Comput.-aided Des. Integr. Circuits Syst.*, 25(6):1000–1010, June 2006.

[17] Farrokh Vatan and Colin Williams. Optimal quantum circuits for general two-qubit gates. *Phys. Rev. A*, 69(3), March 2004.

[18] G Vidal and C M Dawson. Universal quantum circuit for two-qubit transformations with three controlled-NOT gates. *Phys. Rev. A*, 69(1), January 2004.

[19] Henry Zou, Matthew Treinish, Kevin Hartman, Alexander Ivrii, and Jake Lishman. LightSABRE: A lightweight and enhanced SABRE algorithm. 2024.

A Reliable convergence of 4-qubit and 6-qubit systems

As in the case of two qubit systems, we analyze the convergence of (a) random target unitaries, (b) the same target unitary initialized with different sets of parameters, for four qubit and six qubit systems. In (a), we pick five random target unitaries and run the algorithms for all of them till the cost function converges, indicating that the circuit now represents the target. For (b), we choose five different initializations for the same target unitary and compare the convergences.

A.1 4-qubit system

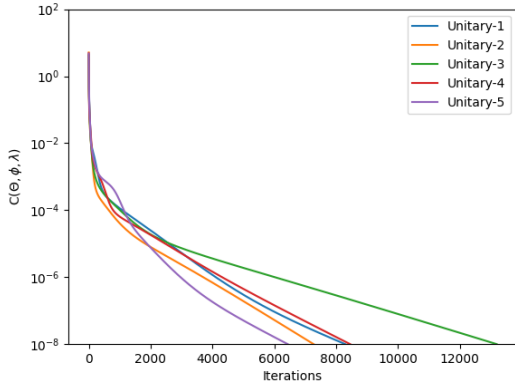


Figure 3: Convergences of five random 16×16 target unitaries optimized through the gradient-based algorithm for $\ell = 32$. The y-axis is in log scale.

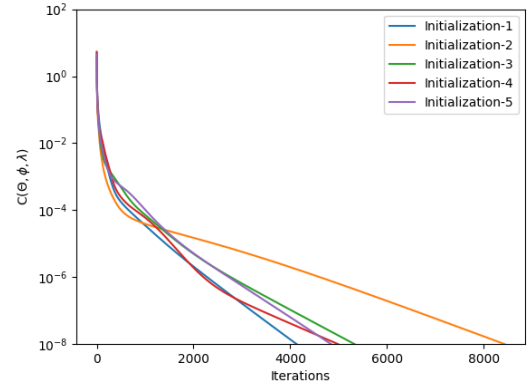


Figure 4: Convergences of the same 16×16 target unitary initialized with five different sets of parameters for $\ell = 32$. The y-axis is in log scale.

A.2 6-qubit system

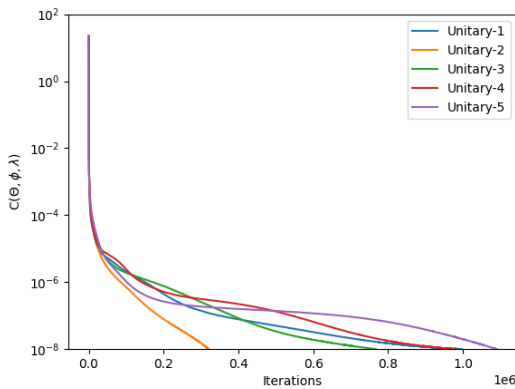


Figure 5: Convergences of five random 64×64 target unitaries optimized through the gradient-based algorithm for $\ell = 341$. The y-axis is in log scale.

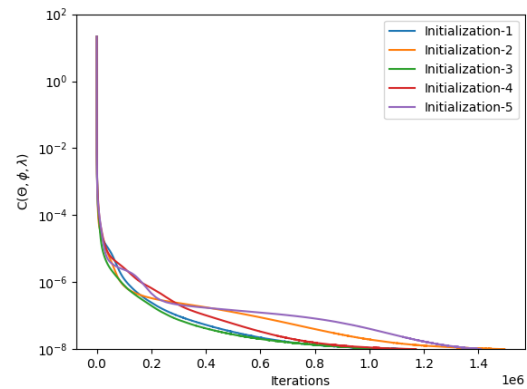


Figure 6: Convergences of the same 64×64 target unitary initialized with five different sets of parameters for $\ell = 341$. The y-axis is in log scale.

Both analyses give the following conclusion: The method robustly finds the circuit for any generic unitary regardless of initial parameters.

B Underparameterized Circuits

After ensuring that we can find a circuit with sufficient accuracy in the case of adequate number of layers, the next objective becomes minimizing the number of CNOTs in the constructed circuit. For this, we study the underparameterized regime for bigger systems, examining its effect on convergence. The goal is to determine whether convergence can still be achieved with fewer parameters, potentially reducing the CNOT count and improving practical implementability. To this end, we explore the underparameterized circuits for the four-qubit and six qubit system. It is important to note that for six qubit systems, the definition of an underparameterized circuit is refined by the choice of circuit topology as well. We observe that the cost function plateaus at $\approx 10^{-3}$ in the best case for underparameterized circuits, which is well before reaching the desired precision of 10^{-8} , even when the number of layers is only slightly short of the required number. As the benefit in the reduction of gates does not compensate well enough for the loss in precision, we conclude that underparameterization is not very useful. Additionally, we look at circuits that are slightly over-parameterized. Interestingly, the over-parameterized circuits converge faster than the adequately parameterized circuits, suggesting that a small parameter surplus aids in convergence.

Thus, our final conclusion is that the success of optimization is guaranteed under adequate parameterization, and the underparameterized circuits fail to converge (see figures 7 and 8).

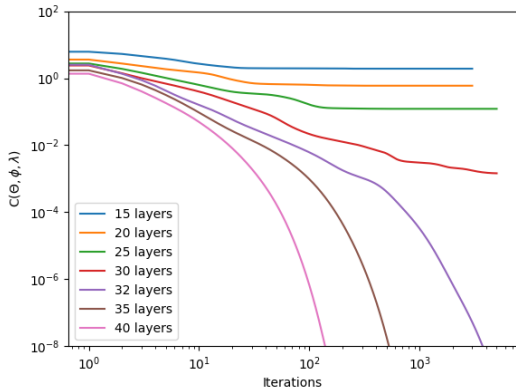


Figure 7: Convergences of the same 4 qubit (16×16) target unitary for different ℓ values. Both x-axis and y-axis are in log scale to aid in comparing various ℓ values.

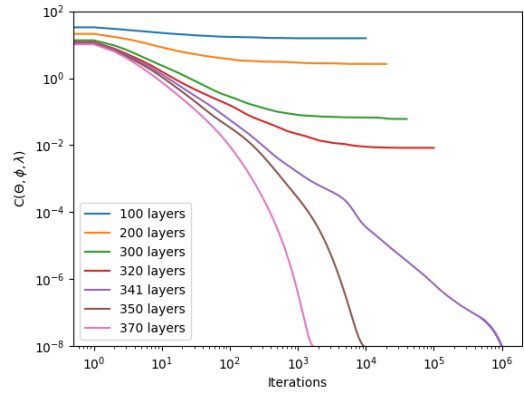


Figure 8: Convergences of the same 6 qubit (64×64) target unitary for different ℓ values. Both x-axis and y-axis are in log scale to aid in comparing various ℓ values.

B.1 Other optimization techniques

Given that simple gradient descent (or our accelerated variant, see Section 3.2.1) failed to find circuits of useful precision at even very mild underparameterization, a natural question was whether more advanced search strategies could succeed. While there are many approaches and algorithms to investigate for this hard problem, our experiments focused on whether a straightforward *modification or extension* of gradient descent could suffice. The most obvious way to do this seemed to be allow modification of the CNOT topology during search. We did brief investigations into several related variants.

- Periodically during optimization, a CNOT layer is exchanged for a different arrangement. If the reconstruction accuracy improves, keep it.
- Alternately: keep it with some other probability, even if the accuracy worsens. This is a form of simulated annealing, and the acceptance probability should reduce towards zero in order to ensure convergence.

- Or as another possibility, instead of allowing an arbitrary CNOT change, only allow changes that don't create underparameterized "redundant" configurations.
- At a given step, instead of trying just one alternate CNOT configuration, try every change at every level, to see if there is any similar CNOT configuration that improves.
- Instead of just changing the CNOT layer, change the CNOT, then re-fit across several steps of gradient descent. If this is better than the original circuit, then accept. This would allow for changes that overall improve, but require parameter adjustments to work.
- Instead of just changing one CNOT layer, scramble the CNOTs and all single-qubit unitaries on a pair of adjacent layers, and re-fit them all; see if this produces an improved circuit. If it does, accept.

None of these seemed to provide a noticeable improvement over the simple gradient descent searches. It seems very difficult to make discrete jumps in topology cooperate with the continuous nature of gradient descent, and so we believe that approaches like continuous relaxations of circuit topologies are likely more promising in this regard.

C Circuits with low connectivity

We investigate two representative cases of low connectivity, which are sub-systems of the 127-qubit IBM chip (see figure 9). The immediate significance of low connectivity is that not all qubits are connected to each other, which means there is a reduction in the total number of parameters in the circuit in a given layer. Nevertheless, as long as the circuit remains adequately parameterized (by increasing the number of layers), there is no fundamental reason to expect a failure of the optimization. Note that since the total number of parameters remains the same, the increase in the number of layers has no effect on the required number of gates.

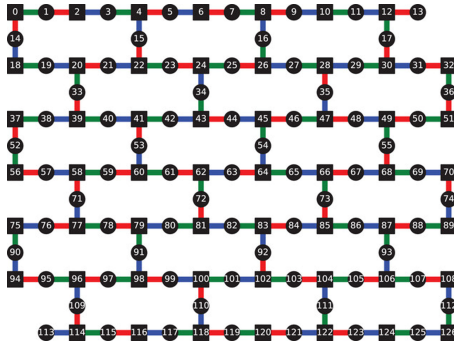


Figure 9: 127 qubit IBM Chip, Adv Quantum Tech, Volume: 8, Issue: 1, First published: 09 October 2024, DOI: (10.1002/qute.202400239)

C.1 Case 1: Qubits 3,4,5,15

We consider qubits 3, 4, 5, and 15 of the chip with the following connectivity constraint: qubit 4 can only be coupled to one of 3, 5, or 15 at the same time; and 3, 5, and 15 are not connected to each other. Effectively, we now have two single-qubit unitaries and one CNOT in each layer. Consequently, the minimum number of layers required for convergence becomes 64. The circuit structure is illustrated in figure 10.

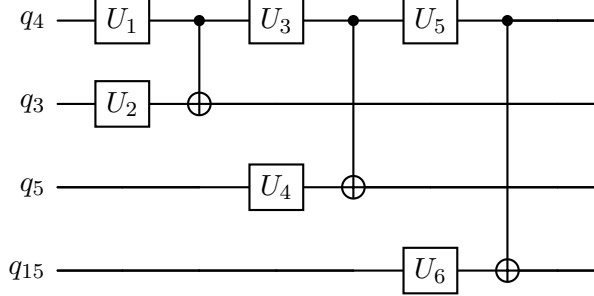


Figure 10: Circuit decomposition for a 16×16 unitary that respects connectivity constraints of qubits 3,4,5,15.

As before, the graphs 11 and 12 discuss the reliable convergence in the case of random target unitaries and the same unitary with different initializations respectively. Meanwhile, graph 13 discusses the saturation of the cost function in the case of underparameterization and presents a few cases of adequate parameterization for comparison. Convergence is reliable with sufficient parameterization, whereas underparameterized circuits cause the cost function to plateau.

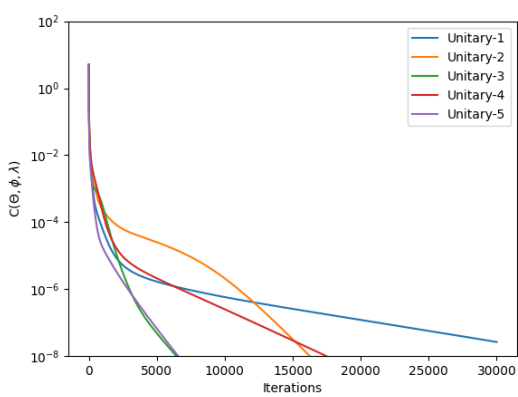


Figure 11: Convergences of five random 16×16 target unitaries for $\ell = 64$ with the y-axis in log scale. The decomposition respects the hardware constraints imposed for qubits 3,4,5,15.

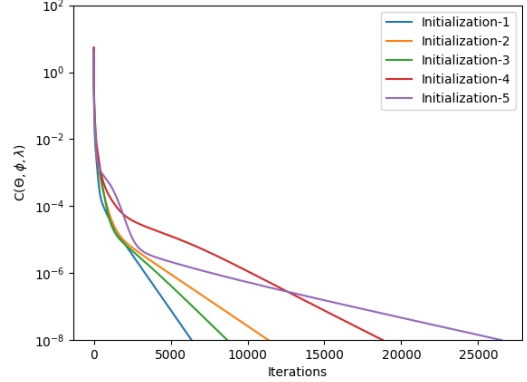


Figure 12: Convergences of the same 16×16 target unitary initialized with five different sets of parameters for $\ell = 64$. The y-axis is in log scale. The decomposition respects the hardware constraints imposed for qubits 3,4,5,15.

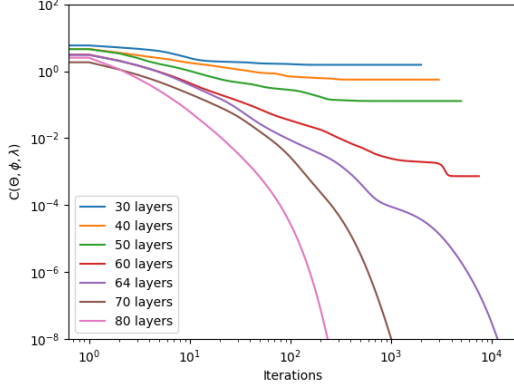


Figure 13: Convergences of the same 16×16 target unitary for different ℓ values. The decomposition respects the hardware constraints imposed for qubits 3,4,5,15. Both x-axis and y-axis are in log scale to aid in comparing various ℓ values.

C.2 Case 2: Qubits 0,1,2,3

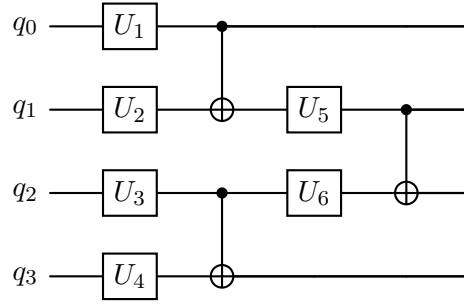


Figure 14: Circuit decomposition for a 16×16 unitary that respects connectivity constraints of qubits 0,1,2,3.

Next, we consider qubits 0,1,2,3 with the following connectivity constraint: only adjacent qubits can be connected, and each can be connected to only one other qubit at a time. The circuit is as shown in figure 14 with $\ell = 42$ and the results are illustrated in the three graphs below.

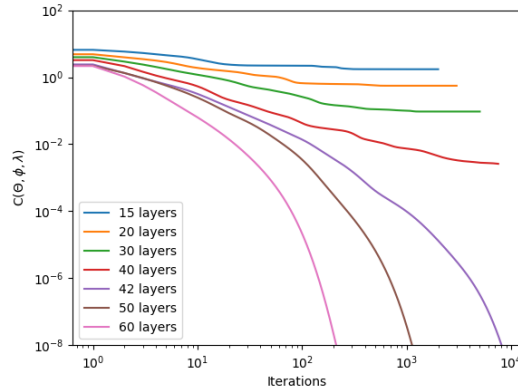


Figure 15: Convergences of the same 16×16 target unitary for different ℓ values. The decomposition respects the hardware constraints imposed for qubits 0,1,2,3. Both x-axis and y-axis are in log scale to aid in comparing various ℓ values.

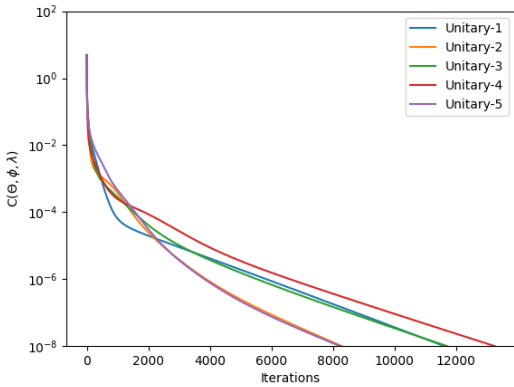


Figure 16: Convergences of five random 16×16 target unitaries for $\ell = 42$ with the y-axis in log scale. The decomposition respects the hardware constraints imposed for qubits 0,1,2,3.

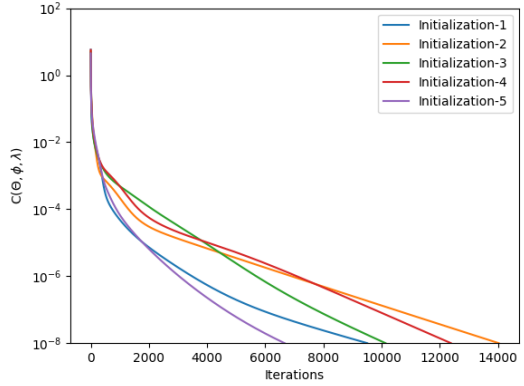


Figure 17: Convergences of the same 16×16 target unitary initialized with five different sets of parameters for $\ell = 42$. The y-axis is in log scale. The decomposition respects the hardware constraints imposed for qubits 0,1,2,3.

Thus, we can conclude that even in the case of a decomposition with low connectivity, we obtain reliable convergence, regardless of initial parameters, as long as there is adequate parameterization—the cost function plateaus in the case of underparameterization.

D Calculation of Failure Probability in Random Circuits

We hypothesize that a poor pairing structure can explain all the failures observed in [3]. To corroborate this, we can see whether theory correct replicates the frequency of failures. For a given circuit topology, we can compute its effective parameters using the principles outlined above. Then if this effective parameter count is less than $4^n - 1$, failure is (generically) necessary.

Any block of three CNOTs coupling the same pair of qubits in a row creates an arbitrary two-qubit gate, giving only 15 parameters instead of the $6 + 4 \cdot 3 = 18$ we would hope for, losing us three effective parameters. Any subsequent gates will lose another 4. Similarly, a block of sufficiently many CNOTs that keeps coupling the same set of three qubits will max out at $4^3 - 1 = 63$. For CNOTs on an $n = 3$ circuit, we can reasonably work this out in closed form.

With $N = 14$ CNOT gates (using the notation of [3] - see their Figure 2), any triple repeat will lead to underparameterization, so we count length-14 words on ABC with no triple letter. This gives a success rate of $\frac{1526976}{3^{14}} \approx 31.9\%$. When $N = 15$, we can have at most one triple repeats, but no quadruple string, giving $\frac{10040832}{3^{15}} \approx 69.98\%$. And repeating the calculation for $N = 16$, we can have a triple repeat or quadruple repeat, but no two, giving $\frac{37327104}{3^{16}} \approx 86.7\%$ success rate. This agrees very well with the numbers reported in [3].

For larger n , the case work on different ways to assign qubits and expected numbers of qubits in different blocks becomes unwieldy to do on paper, but is easily calculated by a computer program. We find excellent agreement with the theory; for $n = 4$, a $< 1\%$ success chance with $N = 61$ CNOT gates, a $\tilde{50}\%$ success rate for $N = 64$, and high success rates for $N \geq 67$. The $n = 5$ agreement is similar.